Title

A visual bio-barcode immunoassay for sensitive detection of triazophos based on biochip silver staining signal amplification

Authors

Wang, Yuanshang
Du, Pengfei
El-Aty, AM Abd
et al.

Publication Date

2021-06-01

DOI

10.1016/j.foodchem.2021.129024

Peer reviewed

HHS Public Access

Author manuscript

Food Chem. Author manuscript; available in PMC 2022 November 10.

Published in final edited form as:

Food Chem. 2021 June 15; 347: 129024. doi:10.1016/j.foodchem.2021.129024.

A visual bio-barcode immunoassay for sensitive detection of triazophos based on biochip silver staining signal amplification

Yuanshang Wang[a], **Pengfei Du**[b,*], **A. M. ABD EL-ATY**[c,d], **Ge Chen**[a], **Huiyan Jia**[e], **Xueyan Cui**[a], **Emel Oz**[f], **Yudan Zhang**[a], **Xiuyuan Zhang**[a], **Guoxin Qin**[g], **Feiyan Yan**[g], **Jing Wang**[a], **Maojun Jin**[a,h,*], **Bruce D. Hammock**[h]

[a]Institute of Quality Standard and Testing Technology for Agro-Products, Key Laboratory of Agro-Product Quality and Safety, Chinese Academy of Agricultural Sciences; Key Laboratory of Agro-Product Quality and Safety, Ministry of Agriculture, Beijing 100081, P. R. China

[b]Institute of Agro-Food Science and Technology Shandong Academy of Agricultural Sciences, Key Laboratory of Agro-Products Processing Technology of Shandong Province, Key Laboratory of Novel Food Resources Processing Ministry of Agriculture, Jinan 250100, China

[c]Department of Pharmacology, Faculty of Veterinary Medicine, Cairo University, 12211 Giza, Egypt

[d]Department of Medical Pharmacology, Medical Faculty, Ataturk University, 25240, Erzurum, Turkey

[e]Ningbo Academy of Agricultural Sciences, Ningbo 315040, PR China

[f]Department of Food Engineering, Faculty of Agriculture, Ataturk University, 25240, Erzurum, Turkey

[g]Agro-products Quality Safety and Testing Technology Research Institute, Guangxi Academy of Agricultural Sciences, Nanning 530007, PR China

[h]Department of Entomology & Nematology and the UC Davis Comprehensive Cancer Center, Davis, CA 95616, USA

Abstract

Herein, a novel visual method for detecting triazophos based on competitive bio-barcode immunoassay was described. The competitive immunoassay was established by gold nanoparticles (AuNPs), magnetic microparticle (MMPs) and triazophos, combined with biochip hybridization system to detect the residual of triazophos in water and apple. Because AuNPs carried many bio-barcodes, which hybridized with labeled DNA on the biochip, catalyzed signal amplification using silver staining was detected by grayscale values as well as the naked eye. Notably, the grayscale values decreases with increasing the concentrations of triazophos, and the color change weakened gradually. The detection range was in between 0.05–10 ng/mL and the minimum detection limit was set at 0.04 ng/mL. Percent recovery calculated from spiked water and apple samples ranged between 55.4–107.8% with relative standard deviations (RSDs) of 12.4–24.9%.

[*]**Corresponding authors: Pengfei Du**, dupengfei2011@163.com, **Tel.**:+86-531-6665-9860., **Maojun Jin**, jinmaojun@caas.cn, **Tel.**: +86-10-8210-6570.

It has therefore been shown that this protocol provides a new insight for rapid detection of small molecule pesticides in various matrices.

Keywords

Bio-barcode; Biochip silver staining; Immunoassay; Triazophos; Gold nanoparticles

1. Introduction

Triazophos, one of the moderately toxic, broad-spectrum, non-systemic organophosphate pesticides, is extensively used in large quantities worldwide to effectively control various pest to agricultural products (Bhandari, Zomer, Atreya, Mol, Yang, & Geissen, 2019; Chen, Liu, & Jiao, 2016; Sapahin, Makahleh, & Saad, 2019). Although, triazophos has been banned for use in agriculture in several countries, including EU and China (Fang et al., 2015; Li et al., 2018), owing to its toxicity and environmental impact; residues can still be detected in agro-products. Therefore, residue detection requires not only a uniform method that can provide quantification under conventional conditions, but also it should meet the requirement for trace detection with high sensitivity (Guo et al., 2018; Huang, Zhao, Wang, & Zhu, 2020).

With the advancement of technology, the current methods for monitoring organophosphates (OPs) are becoming increasingly important. Analytical methods based on chromatographic techniques such as gas chromatography (GC) or liquid chromatography (LC) coupled to mass spectrometry detectors are used for separation and quantification (Ernst, Röder, Tjan, & Jansen, 2020; Laski & Watts, 1973; Ly, Ho, Behra, & Nhu-Trang, 2020; Pang et al., 2020). Although, these methods are accurate and sensitive, they are technically time-consuming, laborious, requiring trained laboratory personnel, and expensive instruments and equipment. On the other hand, rapid techniques based on biological detection, such as immunoassay, enzyme inhibition method, biosensors, have attracted great attention in pesticide residues, owing to their high efficiency and rapid analysis (Chen et al., 2015; Jain, Yadav, Joshi, & Kodgire, 2019; Liu et al., 2018; Y. Liu, Liu, Boroduleva, Eremin, Guo, & Zhu, 2016; Zhang et al., 2017).

Bio-barcode immunoassay, a new emerging technique with high sensitivity, simple operation, and low cost, has been widely used for detection of large (such as DNA and proteins) as well as small (such as environmental pollutants, biotoxins, and pesticides) molecules. In 2003, Chad Mirkind et al. (Nam, Thaxton, & Mirkin, 2003) was the first to introduce the bio-barcode immunoassay for detection of prostate-specific antigen. Later on, the method was improved and used for detection of interleukin 2 (IL-2) (Nam, Wise, & Groves, 2005). A continuous improvement of the assay performance has been observed during recent years that lead to its application in clinical diagnosis and detection of macromolecules, such as C-reactive protein (CRP), bluetongue virus, and hepatitis B virus (HCV) (Broto, Galve, & Pilar Marco, 2017; Yin et al., 2017; Yin et al., 2011). Since small molecules are not suitable for the sandwich assay, the immune competition mode has been adopted instead. By changing the reaction mode, Du et al. (Du et al., 2016)

have developed a fluorescence-based quantitative PCR immunoassay for bio-coding of triazophos. On this basis, Cui et al. (Cui et al., 2019) established a droplet digital polymerase chain reaction-based immunoassay for determination of triazophos in apple, rice, cabbage, and cucumber. However, as the aforementioned methods require PCR equipment, it is difficult for general laboratories to accommodate such incorporation. To enhance the effectiveness of the method, Du et al. (Du et al., 2017) then designed an enzyme-labeled gold nanocomposite probe and constructed a bio-barcode assay using horseradish peroxidase coloration. To explore the development of immunoassays for multi-residue detection, Zhang et al. (Zhang et al., 2018) have used fluorescent markers instead of horseradish peroxidase to design a triazophos single-residue bio-barcode immunoassay method. Furthermore, they have fabricated a fluorometric bio-barcode immunoassay for detection of triazophos residue in agricultural products and water samples using iterative cycles of DNA-RNA hybridization and dissociation of fluorophores by Ribonuclease H (Zhang et al., 2020). Moreover, Zhang et al. (Zhang et al., 2020) selected 6-FAM, Cy3, and Texas red (fluorophores with high fluorescence intensity and small crossover of excitation and emission wavelengths) as oligonucleotide chain markers to design a multi-residue immunoassay for determination of triazophos, parathion, and chlorpyrifos. Other researchers have also explored the quantitative detection of small molecules, such as T-2 toxins and polychlorinated biphenyls (PCBs) on the basis of competitive reaction patterns (Yang, Zhuang, Chen, Ping, & Bu, 2015; Zhang et al., 2018).

Miniaturization technology, with its merits of high throughput, multiple detection, and low cost, has become of increasing importance in environmental and agricultural analysis. In particular, biochips have been frequently used for determination of genes, proteins, and metal ions (Dou, Macias, Shen, Dien Bard, Domínguez, & Li, 2019; Goh & Borisenko, 2017; Kraus et al., 2011; Wu et al., 2014). Biochips are *miniaturized* assemblies arranged on solid substrates and other carriers through planar microfabrication technology. It is possible to immobilize thousands of biomolecules through chemical groups and accurately detect ultra-trace amounts of biomolecules.

Therefore, to design a detection technique for small molecules of pesticides, we developed a highly sensitive immunoassay method based on biochip and silver staining technology for visual detection of pesticide residues (Scheme 1).The monoclonal antibody to triazophos pesticide was assembled onto the surface of gold nanoparticle mainly by electrostatic force. The *thiol-modified* single-*stranded DNA* molecules can bind to the surface of gold nanoparticles by Au-S bonding, and the bio-barcode (complementary to the thiol-modified DNA capture strand) was assembled onto the surface of the gold nanoparticles by hybridization reaction to form the AuNPs. The small molecule hapten (THBu) of the target analyte (triazophos) coupled to the carrier protein (OVA) was covalently bound onto the surface of the magnetic particle to form MMP via a carboxy-amino reaction. When the target pesticide exists in a sample, the magnetic probe and the target pesticide are competing for *antibody binding* sites located on the surface of the AuNPs. Then they are separated by a magnetic field, and release the bio-barcode under high temperature conditions. The released bio-barcode hybridizes with the DNA labeled on the chip, and a silver staining reagent was added to generate a signal amplified by silver staining to provide the quantitative detection of the bio-barcode and the quantitative detection of triazophos.

2. Materials and method

2.1. Materials and reagents

Potassium carbonate (K_2CO_3), sodium hydroxide (NaOH), sodium bicarbonate ($NaHCO_3$), di-potassium hydrogen phosphate (KH_2PO_4), disodium hydrogen phosphate (Na_2HPO_4), anhydrous magnesium sulfate ($MgSO_4$), sodium chloride (NaCl), potassium chloride (KCl), Tween-20 were provided by Sinopharm Chemical Reagent Co., Ltd. (Beijing, China). Chloroauric acid hexahydrate ($HAuCl_4{\cdot}6H_2O$), anhydrous sodium citrate, and bovine serum albumin (BSA) were procured from Sigma-Aldrich (St. Louis, MO, USA). Ovalbumin (OVA), goat anti-mouse IgG-HRP was procured from Jackson ImmunoResearch (West Baltimore Pike West Grove, Pennsylvania, USA), N,N-Dimethylformamide (DMF), 2-(N-morpholino)-ethanesulfonic acid (MES), polyethylene glycol 20,000 (PEG 20,000), N,N-dicyclohexylcarbodiimide (DCC), and Tris-EDTA (TE) buffer (pH 7.4) were acquired from Solarbio (Beijing, China). 3,3′,5,5′-Tetramethylbenzidine (TMB) was purchased from TransGen Biotech (Beijing, China).Tris (2-carboxyethyl) phosphine (TCEP) and 0.2 × SSC washes (containing 0.1% SDS) were secured from Takara (Kusatsu, Japan). The silver enhancer solution A and solution B were supplied by Academy of Military Medical Sciences (Beijing, China). Hybridization buffer was bought from Roche (Diagnostics GmbH, Mannheim, Germany). Nitric acid and concentrated hydrochloric acid were provided by Beijing Chemical Reagent Factory (Beijing, China). HPLC-grade acetonitrile (ACN), methanol, n-hexane, and acetone were procured from Thermo Fisher Scientific (MA, USA). Octadecyl (C_{18}, 40−60 μm), primary-secondary amine (PSA), and graphitized carbon black (GCB, 120−400 mesh) were obtained from Bonna-Agela Technologies (Tianjin, China). MMPs (10 mg/mL) modified with carboxyl (−COOH) groups were secured from Invitrogen (Grand Island, NY, USA). The *haptenated* protein (THBu-OVA) and monoclonal antibodies (mAbs) (4.53 mg/mL) were *generously* donated by the Institute of Pesticide and Environmental Toxicology (Zhejiang University, Zhejiang, China). Triazophos analytical standard (purity: 98%) was obtained from Dr. Ehrenstorfer GmbH (Augsburg, Germany). According to the detection requirements, 4 DNA base sequences were designed as shown in Table 1, (A) thiol-modified DNA capture chain, (B) bio-barcode DNA strand, (C) DNA chain of aminated capture probe fixed on chip, and (D) detection probe DNA strand. All oligonucleotides were generated by Shanghai Sangon Biotech Co., Ltd. (Shanghai, China).

2.2. Functionalization of AuNPs

The AuNPs used in this study were prepared as previously described (Nam, Thaxton, & Mirkin, 2003) with some minor modifications. Prior to modification, sulfhydryl group-modified DNA tends to form stable disulfide bonds during synthesis, dissolution, and storage, which requires the use of Tris (2-carboxyethyl) phosphine (TCEP, 20 mmol/L) aqueous solution to reduce the disulfide bond of thiol-modified DNA to the active *sulfhydryl* form. The thiol-modified capture single-stranded DNA was dissolved in TE solution according to the DNA manufacturer's instructions, mixed with TCEP solution at a ratio of 1:200, and then shaken overnight. At the same time, K_2CO_3 was added to the gold nanoparticle solution to adjust the pH to 8.5, then 45 μg of triazophos monoclonal antibody (incubated for 1 h at room temperature with slow oscillation) was added. The thiol DNA capture chain (A) was then added to the above mixture at a final concentration of 1 μmol/L.

After aging for 16 h at 4 °C, the mixture was left undisturbed and then slowly oscillated every 4 h. Afterward, PEG 20,000 was added at a final concentration of 0.5%, and then 1 mol/L NaCl was added at a final concentration of 0.13 mol/L into 6 installments at 4 °C for 24 h, with 30 min interval before the next salt addition. Subsequently, BSA and PEG 20,000 were each added at the final concentration of 0.5% each. After 2 h of quiescence, the mixture was centrifuged at 13,000 rpm/min for 30 min at 4 °C and the supernatant was discarded to remove unmodified antibodies and single-stranded DNA capture strands. The precipitate was redissolved in 1 mL of 10 mmol/L PBS buffer (pH 7.4), containing 2% BSA and 0.1% PEG 20,000. Next, the bio-barcode strands (final concentration 2 μmol/L) were added to the above modified gold nanoparticles mixture, and centrifuged at room temperature for 4 h at 13,000 rpm/min. The supernatant was discarded to remove the unmodified bio-barcode, and then 1 mL 10 mmol/L PBS buffer, (pH 7.4, containing 2% BSA) was added, 0.1% PEG 20,000; the precipitate was resuspended and mixed by gentle blowing with a pipette and stored at 4 °C pending analysis.

2.3. Functionalization of MMPs

The MMPs was functionalized by applying triazophos hapten-OVA modifications onto the surface of the magnetic beads as previously described (Du et al., 2017; Gui, Jin, Chen, Cheng, & Zhu, 2006). The magnetic particles were removed from the supernatant under magnetic conditions, and then washed for 3–4 times with 15 mmol/L MES solution (pH 6.0). Following magnetic separation, the magnetic particles were resuspended in MES solution, to which EDC was added. The mixture was shaken at room temperature for 30 min. The activation solution was then removed under magnetic field, then triazophos hapten-OVA and MES solution were added to the magnetic beads and the reaction mixture was shaken overnight at room temperature. Again under magnetic field, the mixture was washed with PBS containing 0.1% Tween-20 at 3,000 rpm/min for 30 s in 2–3 times. The magnetic beads were then added to PBS buffer containing 2% BSA for 1 h. Finally, the magnetic beads were resuspended in PBS buffer containing 0.1% Tween-20 and 0.1% BSA. The final prepared MMPs were stored at 4°C for backup.

2.4. Biochip preparation

The aminated capture probe designed in the experiment was spotted on the aldehyde-modified glass slide through a chip spotter. The sampling process was conducted according to Yeh, Huang, Chang, Lin, & Lin (2009). The concentration of aminated DNA capture probe was fixed to 75 μmol/L, with a dot diameter of 100 μm, a dot spacing of 500 μm, and spot volume of 0.7 nL at 37 °C. After spotting, the glass slides were allowed to dry at room temperature and relative humidity of 75%. After 72 h, the slides were washed twice with 0.2% SDS and ultrapure water for 2 min per each time, and then blocked with aldehyde-based blocking solution (0.1 g sodium borohydride, 30 mL PBS, 10 mL 99% ethanol) for 15 min. Afterward, the bioslides were placed in a 40 mmol/L mercaptosuccinic acid solution to block the unbound sites on the slides; the blocking step was maintained for 30 min. Subsequently, the slides were washed twice with 0.2% SDS and ultrapure water for 2 min per each time. Finally, the biochips were dried at room temperature and held at 4 °C until used.

2.5. Establishment of bio-barcode immunoassay for sensitive detection of triazophos based on biochip silver staining signal amplification

A 50 μL of 10-fold diluted AuNPs, 20 μL of triazophos standard (or sample) diluted with competitive reaction buffer, and 20 μL of 100-fold diluted magnetic nanoprobe were added to centrifuge tube and then incubated for 15 min at 37°C with vigorous shaking. Subsequently, through the separation of the magnetic field, PBS solution was used at least three times to remove unbound antigen and hapten. Next, 60 μL of ultrapure water was added with vigorous shaking at 60 °C for 1 h to dehybridize the bio-barcode DNA under high temperature and low salt conditions; supernatant was collected after magnetic separation. After the release of the bio-barcode, the supernatant was transferred to a clean microcentrifuge tube by magnetic separation, and centrifuged at 13,000 rpm/min for 10 min. Then, 4 μL of supernatant was transferred to a microcentrifuge tube containing 15 μL of detection probe DNA (D) that was mixed by shaking. This mixture was dropped onto the biochip, hybridized at 48 °C for 2 h. The reaction solution was removed and the biochip was washed with 0.2×SSC. After drying, a mixture of 20 μL of silver enhancer solution A and B was evenly dripped onto the biochip and the reaction was held in the dark at room temperature. A 9 min later, the reaction was terminated by placing it in deionized water. After this rinse, it was dried and the detection result can be read out through the grayscale value of the image using chip scanner, or it can be directly judged by naked eye observation.

2.6. Establishment of indirect ELISA

The activity of AuNPs and triazophos antibody was compared using indirect ELISA as following: a volume of 100 μL (per well) of OVA-THBu solution diluted with 0.05 mol/L CBS(carbonate buffer, pH 9.6) to 10 μg/mL was added to a 96-well transparent plate and then incubated at 37°C for 2 h. Afterwards, the coating solution was discarded, and the transparent plate was washed three times with PBST (0.01 mol/L, pH 7.4) to remove the remaining washing solution. Thereafter, 300 μL of PBS buffer containing 2% skimmed milk was added to each well, blocked overnight at 4 °C. After the blocked transparent plates were restored to room temperature, they were washed three times with PBST to remove the remaining blocking solution. Next, 100 μL of antibody or AuNPs (diluted with 5% BSA in 0.01 mol/L, pH 7.4 PBS buffer) was added to each well and then incubated at 37 °C for 1 h. The reaction solution was discarded and the transparent plates were washed again three times with PBST. A 100 μL of enzyme-labeled secondary antibody (goat anti-mouse IgG-HRP) diluted 10000 times with 0.01 mol/L PBS immunoreactions buffer containing 5% BSA was added to each well and incubated at 37 °C for 1 h. Later, the reaction solution was discarded and the plate was washed 5 times with washing buffer. A 100 μL of TMB solution was added to each well and then incubated at 37 °C in the dark with gentle shaking. After 15 min, 100 μL of 2 mol/L sulfuric acid was added to each well to stop the reaction, and the absorbance was measured at 450 nm with a multifunctional microplate reader.

2.7. Establishment of direct competition ELISA

After incubation for 2 h at 37 °C with 100 μL of diluted triazophos antibody solution in each well of a 96-well enzyme labeled plate, the transparent plates were washed 3 times with 0.01 mol/L PBST (pH 7.4). After restoring the enzyme labeled plate to room temperature, the

remained washing solution was removed and 300 μL of PBS (containing 2% skimmed milk) was added per each well blocked at 4 °C overnight. After blocking, the transparent plates were washed twice to remove any residual sealing solution, then 50 μL triazophos or sample and 50 μL of enzyme-labeled hapten (0.2 mg/L) were added and incubated at 37°C for 1 h. The reaction solution was discarded and the transparent plates were washed at least three times to remove the residual washing solution. Thereafter, 100 μL TMB was added to each well and slowly shaken at 37°C away from light. After 15 min, 100 μL 2 mol/L sulfuric acid was added to each well to terminate the reaction and the absorbance value at 450 nm was read with a multifunctional enzyme reader.

2.8. Sample pre-treatment

Water and apple were used as real samples to compare the performance of the developed bio-barcode immunoassay and conventional ELISA. For water sample (10 mL), triazophos was diluted with 0.01 M PBS containing 5% methanol to final concentration of 10, 50, and 100 μg/kg, and measured directly. Blank apple samples procured from local markets located in Beijing (China) were confirmed to be free from the tested analyte by liquid chromatography-mass spectrometry (LC-MS). A homogenized sample (10 g) was weighed into a 50 mL centrifuge tube, to which a standard solution of triazophos was added at a final concentration of 10, 50, and 100 μg/kg. The mixture was left undistributed for 2 h at room temperature. Afterward, 10 mL acetonitrile was added, then vortex-mixed for 30 s. Subsequently, 4 g anhydrous $MgSO_4$ and 1 g NaCl were added, mixed on a vortex® (Scientific Industries, NY, USA) for 30 s, and then centrifuged at 10,000 r/min for 5 min at 4 °C. Next, 2 mL of acetonitrile extract was transferred to another centrifuge tube, to which 50 mg PSA and 50 mg C_{18} were added for purification. The mixture was vortexed for 30 s at 4 °C and then centrifuged at 10,000 rpm/min for 5 min. Supernatant (1 mL) was dried under nitrogen at 30 °C, and the residue was reconstituted in 5% methanol-PBS for detection by both bio-barcode assay and ELISA.

3. Results and discussion

3.1. Characterization and optimization of gold nanoprobes

The ultraviolet wavelength scan results showed in Figure. 1. The unlabeled gold nanoparticles wavelength scan had a maximum absorption peak at 520 nm. Wavelength scans of the AuNPs probe modified with antibody, thiol-capture chain, and bio-barcode showed a red shifted absorption at 526 nm. The UV scan indirectly indicated that antibodies, thiol-trapping strand DNA, and bio-barcode were assembled onto the gold nanoparticles surface. Transmission electron microscopy (TEM) results showed Figure. 1 that the nanogold before and after modification was uniform in size and well dispersed, the synthesized AuNPs had a narrow size distribution with an average diameter of 15 nm, SD=0.74 with no aggregation before or after reaction. Compared to the pre-modified gold nanoparticles, the modified gold nanoparticles have a halo ring around the particles, which indicates that a low electron density material was encapsulated on the surface of the gold nuclei. Furthermore, this phenomenon indirectly demonstrated the presence of antibodies and nucleic acids adsorbed onto the gold nanoparticles surfaces.

3.2. pH optimization in the immobilization of the antibody

To ensure the maximum degree of antibody adsorption, it was found that in the preparation of AuNPs depends critically on pH. A 100 μL gold nanoparticle solution was added to each microtube, and the pH was adjusted to 6.5, 7.0, 7.5, 8.0, 8.5, and 9.0, respectively. Then 10 μL of 4.53 mg/mL monoclonal antibody was added to each well, and after with standing for 30 min, 10 μL of 10% NaCl solution was added to each well. After NaCl titration, let it stand for 2 h, and the results are shown in the Figure. 2. Probes with pH values of 6.5, 7.0, 7.5, and 8.0 agglutinated and turned blue, while the nano-gold solutions with pH values of 8.5 to 9.0 remained red. Among them, the well with the lowest pH value that keeps the color unchanged is considered as the optimal pH value for antibody adsorption of AuNP. Therefore, a pH of 8.5 was selected as the optimal pH for the gold nanoparticles.

3.3. Optimization of antibody addition in the synthesis of AuNPs

After the antibodies were modified on the surface of the gold nanoparticles, an electric double layer was formed. If the amount of added antibody added was insufficient, the salt ions in the solution would disrupt the electronic balance. However, when the amounts of antibodies were just appropriate, the antibodies modified on the surface of the nanogold effectively prevent the agglomeration of nanogold. The optimal amount of antibody adsorbed onto the gold nanoparticles was determined by NaCl titration, and the results are shown in Figure. 3. The concentration of fixed antibodies was 0.27 mg/mL, and the volumes of added antibodies were 1, 2, 3, 4, 5, 6, and 7 μL, respectively. The amount of antibody in between 1–5 μL was not enough to stabilize the nano-gold, and different degrees of red and blue aggregation would occur. On the other hand, when the amount of added antibody was 6 or 7 μL, the color of the solution does not change. The least amount of antibody to maintain the color unchanged is considered the optimum for stabilizing the nanogold. The actual amount of nanogold modified antibody used in the actual experiment was 120% of the above optimal use. Therefore, the optimal protein dosage of 200 μL nanogold was 2.3 μg.

3.4. Detection of surface antibody activity on AuNPs

We used an indirect ELISA method to analyze the activity of triazophos antibody before and after modification. As shown in Figure. 4, the activity of the antibodies before and after labeling of the AuNPs was basically consistent with the absorbance value at 450 nm, the finding which denotes that the synthesis process of the AuNPs did not affect the activity of the antibodies.

3.5. Optimization of competitive detection reaction

Methanol is a widely used organic solvent for dissolving pesticide standards, such as triazophos. Therefore, it is necessary to investigate the effect of methanol concentration in buffer on the immunoassay. PBS solution containing 1, 5, 10, 15, and 20% methanol were formulated separately and were used to dilute pesticide standards (5 ng/mL) to detect grayscale values. As shown in Figure. S1, when PBS solution contains less than 5% methanol, the grayscale value increases as the concentration of methanol increased; the finding which is in line with others (Li, Hua, Ma, Liu, Zhou, & Wang, 2014). This means that certain concentration of methanol can promote the affinity of the antibodies

to triazophos and THBu-OVA on the AuNPs. When the concentration exceeded certain values, the organic solvent would exhibit a negative impact on the reaction system and thus the grayscale value decreases. Hence, 5% methanol has been chosen as the optimum concentration in PBS buffer.

According to a previous study (Chen et al., 2019), the amount of antibody and hapten-OVA had an important impact on the performance of immune competition methods. To establish a bio-barcode immunoassay for sensitive detection based on biochip, an orthogonal test method was used to design a series of AuNPs with dilution ratios of 10, 20, 40, 80, and 100 times, and MMPs with dilution ratio of 20, 40, 80, 100, and 150 times, respectively. The results are shown in Table S2. The optimum working concentration of AuNPs and MMPs was determined based on the ratio (Gmax/I) value of the maximum grayscale value to pesticide concentration (IC_{50}) at 50% inhibition rate. It was finally determined that the dilution factor of the AuNPs was 10 times and that of MMPs was 100 times.

3.6. Optimization of biochip hybridization system

In the biochip hybridization system, the dissociated bio-barcodes were allowed to be with their complementary aminated capture probe DNA (C) and the detection probe DNA (D) through hybridization and silver stain enhancer reagent. The catalytic reduction of silver ions by nanogold was used to wrap the reduced silver ions around the nanogold particles to form a silver shell, which generated an amplified silver stain signal to quantify the bio-barcodes and triazophos residues.

When the content of the detection probe (D) is too low, the hybridization reaction between the bio-barcode, the aminated capture probe DNA assembled on the biochip, and the detection probe (D) would be insufficient, which in turn would reduce the sensitivity of the whole experiment. On the other hand, if the detection probe (D) content is extremely high, a non-specific adsorption of gold nanoparticles may occur in the hybridization reaction, which results in excessive signal intensity and possibly false-positive signals. The concentration of the detection probes was therefore optimized. As can be seen from Figure. S2, the grayscale value of the silver stain increases with the concentration of the detection probe. When the concentration of the detection probe is 11.0 nmol/L, the signal reaches the highest value. Increases in the concentration of the detection probe would increase (non-significant) the signal intensity of the silver staining biochip. Therefore, the optimal concentration of the detection probe in this experiment was set at 11.0 nmol/L. Additionally, the silver staining time was optimized, and the results are shown in Figure. S3. The grayscale increased significantly with increasing time from 0 to 8.5 min, which is slowly increased after 9 min. If the silver staining time continues to rise, the background signal would deepen rapidly, generating false-positive signals and in turn affecting the accuracy of the experiment. Hence, the optimal silver staining time was set at 9 min.

3.7. Establishment of standard curve

Under optimized experimental conditions, we used a bio-barcode immunoassay method based on biochip silver staining technology to detect different concentrations of triazophos standard. When the pesticide concentration was low, the AuNPs bound more MMPs and

may contain more bio-barcodes after de-hybridization. On the other hand, the AuNPs were less tightly bound to MMPs and may contain relatively less bio-barcodes after de-hybridization at higher concentration. As shown in Figure. S4, when the concentration of triazophos was in the range of 0.05–10 ng/mL, the hapten (on the MMPs) competed with pesticide molecule for the active site on the AuNPs.

The log value (LogC) of pesticide concentration was linearly fitted with the inhibition rate.

$$I\% \frac{(Gmax - G\ min) - (Gx - Gmin)}{Gmax\text{-}Gmin} \times 100$$

where "I" represents the rate of inhibition, "G_{max}" represents the grayscale value without pesticide, "G_{min}" represents the grayscale value of the blank control well, "G_x" represents a grayscale value at a pesticide concentration of x.

The affinity of the antibody to a pesticide is indicated by IC_{50} (pesticide concentration with an inhibition rate of 50%) and IC_{10} (pesticide concentration with an inhibition rate of 10%) as the sensitivity of this method. The concentration of triazophos in the range of 0.05–10 ng/mL showed a good linear relationship (LogC) with the rate of inhibition, with a linear regression equation of y=0.34 LogX+0.59 and a correlation coefficient of 0.988. On the other hand, the IC_{50} and IC_{10} were 0.55 and 0.04 ng/mL, respectively. In sum, this immunoassay method can be used as a quantitative method for detection of pesticide residues with high sensitivity.

3.8. Analysis of spiked samples

To investigate the accuracy of the competitive bio-barcode immunoassay method for real samples, triazophos standard was spiked to water and apple samples for recovery test. From Table S1, the recoveries of water samples were ranged from 71.1–105.2% with RSDs in between 12.4%−14.4%; the finding which indicates that the assay method exhibited satisfactory accuracy and precision for detection of water samples. On the other hand, the recovery rate of apple samples was in between 55.4–107.8% with RSDs ranged from15.3% −24.9%.

3.9. Relevance studies

To further evaluate the applicability of this immunoassay method for spiked water and apple samples. From Table S1, we compared the recovery rates obtained by ELISA with this method. The linear regression equations were y=0.98x + 1.81 (x-axis: results of this method; y-axis: results of ELISA determination), with a coefficient of determination of 0.941. The results of this method are well correlated with ELISA.

4. Conclusions

In this study, by constructing two detection probes: AuNPs and MMPs, a biochip hybridization system was designed to design a competitive bio-barcode immunoassay for detection of triazophos. The detection range of the developed method was 0.05–10 ng/mL and the LOD was 0.04 ng/mL. This biochip is rapid and easy to visualize directly

by grayscale value or naked eye. The developed method might have the potential and applicability in the field of rapid detection of small molecule pesticides.

Supplementary Material

Refer to Web version on PubMed Central for supplementary material.

Acknowledgments

This study was financially supported by National Key Research Program of China (No. 2016YFD0401101), NIEHS Superfund Research Program (No. P42 ES04699), and Ningbo Innovation Project for Agro-Products Quality and Safety (No. 2019CXGC007).

References

Bhandari G, Zomer P, Atreya K, Mol HGJ, Yang X, &Geissen V (2019). Pesticide residues in Nepalese vegetables and potential health risks. Environmental Research, 172, 511–521. [PubMed: 30852454]

Broto M, Galve R, & Pilar Marco M (2017). Sandwich NP-based biobarcode assay for quantification C-reactive protein in plasma samples. Analytica Chimica Acta, 992, 112–118. [PubMed: 29054144]

Chen G, Jin M, Yan M, Cui X, Wang Y, Zheng W, . . . Wang J (2019). Colorimetric bio-barcode immunoassay for parathion based on amplification by using platinum nanoparticles acting as a nanozyme. Microchimica Acta, 186(6).

Chen G, Yang L, Jin M, Du P, Zhang C, Wang J, . . . Wang J (2015). The Rapid Screening of Triazophos Residues in Agricultural Products by Chemiluminescent Enzyme Immunoassay. Plos One, 10(7).

Chen W, Liu Y, & Jiao B (2016). Dissipation behavior of five organophosphorus pesticides in kumquat sample during honeyed kumquat candied fruit processing. Food Control, 66, 87–92.

Cui X, Jin M, Zhang C, Du P, Chen G, Qin G, . . . Wang J (2019). Enhancing the Sensitivity of the Bio-barcode Immunoassay for Triazophos Detection Based on Nanoparticles and Droplet Digital Polymerase Chain Reaction. Journal of Agricultural and Food Chemistry, 67(46), 12936–12944. [PubMed: 31670953]

Dou M, Macias N, Shen F, Dien Bard J, Domínguez DC, & Li X (2019). Rapid and Accurate Diagnosis of the Respiratory Disease Pertussis on a Point-of-Care Biochip. EClinicalMedicine, 8, 72–77. [PubMed: 31008450]

Du P, Jin M, Chen G, Zhang C, Cui X, Zhang Y, . . . Wang J (2017). Competitive colorimetric triazophos immunoassay employing magnetic microspheres and multi-labeled gold nanoparticles along with enzymatic signal enhancement. Microchimica Acta, 184(10), 3705–3712.

Du P, Jin M, Chen G, Zhang C, Jiang Z, Zhang Y, . . . Wang J (2016). A Competitive Bio-Barcode Amplification Immunoassay for Small Molecules Based on Nanoparticles. Scientific Reports, 6.

Ernst GF, Röder SJ, Tjan GH, & Jansen JTA (2020). Thin Layer Chromatographic Detection and Indirect Gas Chromatographic Determination of Three Carbamate Pesticides. Journal of AOAC(5), 5.

Fang L, Zhang S, Chen Z, Du H, Zhu Q, Dong Z, & Li H (2015). Risk assessment of pesticide residues in dietary intake of celery in China. Regulatory Toxicology and Pharmacology, 73(2), 578–586. [PubMed: 26344481]

Goh MC, &Borisenko V (2017). Microfluidic biochip and integrated diffractive optics for bacteria growth control and monitoring. Analytical Methods, 9(16), 2392–2396.

Gui WJ, Jin RY, Chen ZL, Cheng JL, & Zhu GN (2006). Hapten synthesis for enzyme-linked immunoassay of the insecticide triazophos. Analytical Biochemistry, 357(1), 9–14. [PubMed: 16920057]

Guo Y, Liu R, Liu Y, Xiang D, Liu Y, Gui W, . . . Zhu G (2018). A non-competitive surface plasmon resonance immunosensor for rapid detection of triazophos residue in environmental and agricultural samples. Science of the Total Environment, 613–614, 783–791.

Huang D, Zhao J, Wang M, & Zhu S (2020). Snowflake-like gold nanoparticles as SERS substrates for the sensitive detection of organophosphorus pesticide residues. Food Control, 108, 106835.

Jain M, Yadav P, Joshi A, &Kodgire P (2019). Advances in detection of hazardous organophosphorus compounds using organophosphorus hydrolase based biosensors. Critical Reviews in Toxicology, 49(5), 387–410. [PubMed: 31268806]

Kraus S, Kleines M, Albers J, Blohm L, Piechotta G, Puettmann C, . . . Nebling E (2011). Quantitative measurement of human anti-HCV Core immunoglobulins on an electrical biochip platform. Biosensors & Bioelectronics, 26(5), 1895–1901. [PubMed: 20400289]

Laski RR, & Watts RR (1973). Gas chromatography of organonitrogen pesticides, using a nitrogen-specific detection system. Journal of AOAC, 56(2), 328–332.

Li M, Hua X, Ma M, Liu J, Zhou L, & Wang M (2014). Detecting clothianidin residues in environmental and agricultural samples using rapid, sensitive enzyme-linked immunosorbent assay and gold immunochromatographic assay. Science of the Total Environment, 499, 1–6. [PubMed: 25173856]

Li Z, Nie J, Yan Z, Cheng Y, Lan F, Huang Y, . . . Li A (2018). A monitoring survey and dietary risk assessment for pesticide residues on peaches in China. Regulatory Toxicology and Pharmacology, 97, 152–162. [PubMed: 29909271]

Liu B, Gong H, Wang Y, Zhang X, Li P, Qiu Y, . . . Zhang C (2018). A gold immunochromatographic assay for simultaneous detection of parathion and triazophos in agricultural products. Analytical Methods, 10(4), 422–428.

Liu Y, Liu R, Boroduleva A, Eremin S, Guo Y, & Zhu G (2016). A highly specific and sensitive fluorescence polarization immunoassay for the rapid detection of triazophos residue in agricultural products. Analytical Methods, 8(36), 6636–6644.

Ly T-K, Ho T-D, Behra P, &Nhu-Trang T-T (2020). Determination of 400 pesticide residues in green tea leaves by UPLC-MS/MS and GC-MS/MS combined with QuEChERS extraction and mixed-mode SPE clean-up method. Food Chemistry, 326, 126928. [PubMed: 32408000]

Nam JM, Thaxton CS, &Mirkin CA (2003). Nanoparticle-based bio-bar codes for the ultrasensitive detection of proteins. Science, 301(5641), 1884–1886. [PubMed: 14512622]

Nam JM, Wise AR, & Groves JT (2005). Colorimetric bio-barcode amplification assay for cytokines. Analytical Chemistry, 77(21), 6985–6988. [PubMed: 16255599]

Pang G, Chang Q, Bai R, Fan C, Zhang Z, Yan H, & Wu X (2020). Simultaneous Screening of 733 Pesticide Residues in Fruits and Vegetables by a GC/LC-Q-TOFMS Combination Technique. Engineering, 6(4), 432–441.

Sapahin HA, Makahleh A, & Saad B (2019). Determination of organophosphorus pesticide residues in vegetables using solid phase micro-extraction coupled with gas chromatography-flame photometric detector. Arabian Journal of Chemistry, 12(8), 1934–1944.

Wu C-C, Ku B-C, Ko C-H, Chiu C-C, Wang G-J, Yang Y-H, & Wu S-J (2014). Electrochemical impedance spectroscopy analysis of A-beta (1–42) peptide using a nanostructured biochip. Electrochimica Acta, 134, 249–257.

Yang G, Zhuang H, Chen H, Ping X, & Bu D (2015). A gold nanoparticle based immunosorbent bio-barcode assay combined with real-time immuno-PCR for the detection of polychlorinated biphenyls. Sensors and Actuators B-Chemical, 214, 152–158.

Yeh C-H, Huang H-H, Chang T-C, Lin H-P, & Lin Y-C (2009). Using an electro-microchip, a nanogold probe, and silver enhancement in an immunoassay. Biosensors and Bioelectronics, 24(6), 1661–1666. [PubMed: 18838263]

Yin H. q., Ji C. f., Yang X. q., Wang R, Yang S, Zhang H. q., & Zhang J. g. (2017). An improved gold nanoparticle probe-based assay for HCV core antigen ultrasensitive detection. Journal of Virological Methods, 243, 142–145. [PubMed: 28189584]

Yin H. q., Jia M. x., Shi L. j., Yang S, Zhang L. y., Zhang Q. m., & Wang S. q. (2011). Nanoparticle-based bio-barcode assay for the detection of bluetongue virus. Journal of Virological Methods, 178(1), 225–228. [PubMed: 21619893]

Zhang C, Du P, Jiang Z, Jin M, Chen G, Cao X, . . . Wang J (2018). A simple and sensitive competitive bio-barcode immunoassay for triazophos based on multi-modified gold nanoparticles and fluorescent signal amplification. Analytica Chimica Acta, 999, 123–131. [PubMed: 29254562]

Zhang C, Jiang Z, Jin M, Du P, Chen G, Cui X, . . . Wang J (2020). Fluorescence immunoassay for multiplex detection of organophosphate pesticides in agro-products based on signal amplification of gold nanoparticles and oligonucleotides. Food Chemistry, 326, 126813. [PubMed: 32438234]

Zhang H, Sun L, Zhang Y, Kang Y, Hu H, Tang H, & Du Y (2017). Production of stable and sensitive SERS substrate based on commercialized porous material of silanized support. Talanta, 174, 301–306. [PubMed: 28738584]

Zhang M, Huo B, Yuan S, Ning B, Bai J, Peng Y, . . . Gao Z (2018). Ultrasensitive detection of T-2 toxin in food based on bio-barcode and rolling circle amplification. Analytica Chimica Acta, 1043, 98–106. [PubMed: 30392674]

Zhang X, Du P, Cui X, Chen G, Wang Y, Zhang Y, . . . Hammock B (2020). A sensitive fluorometric bio-barcodes immunoassay for detection of triazophos residue in agricultural products and water samples by iterative cycles of DNA-RNA hybridization and dissociation of fluorophores by Ribonuclease H. Science of the Total Environment, 717, 137268. [PubMed: 32084695]

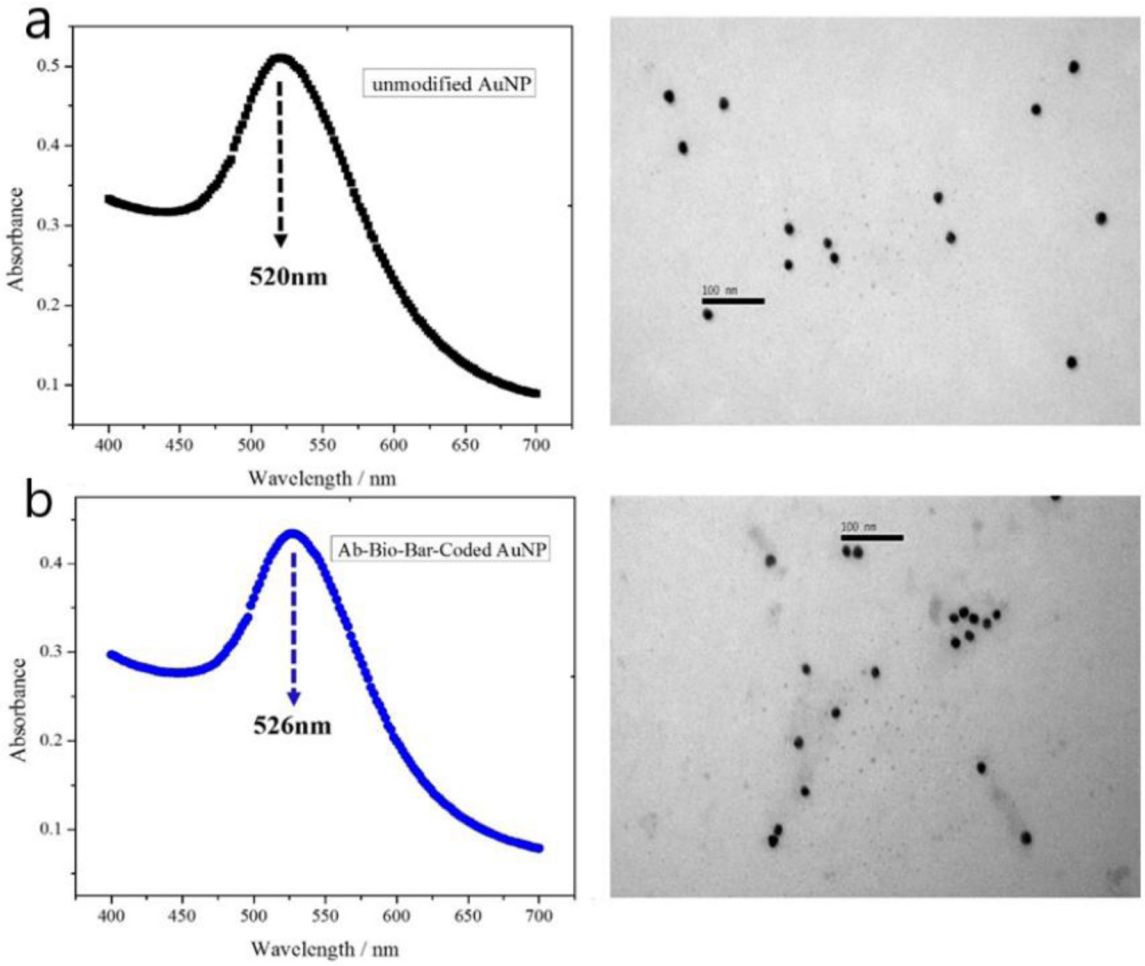

Fig. 1.

(a).The UV spectra and TEM images of gold nanoparticles before labeling. (b). The UV spectra and TEM images of gold nanoparticles after labeling.

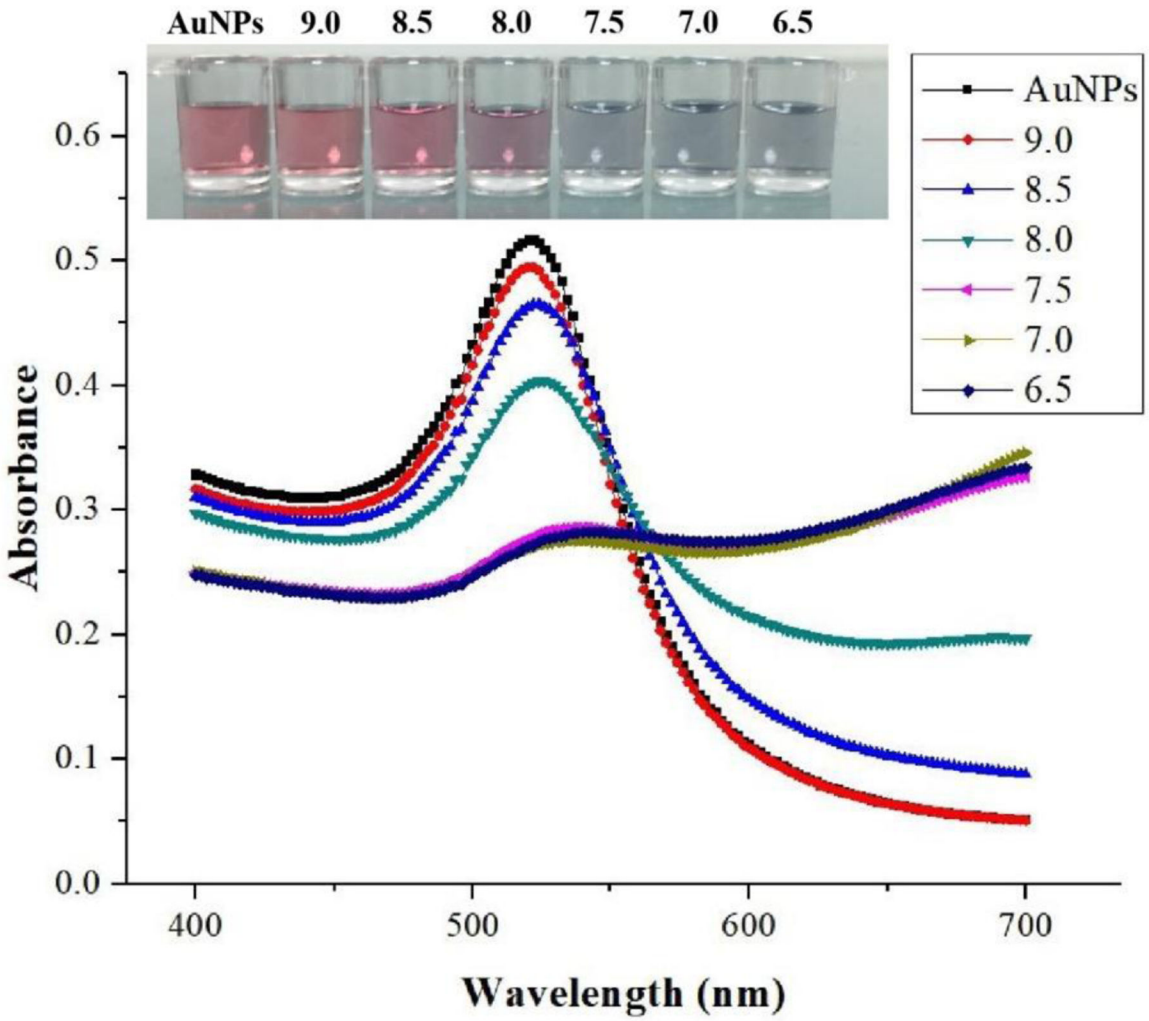

Fig. 2.
Optimization of the pH of AuNPs probes.

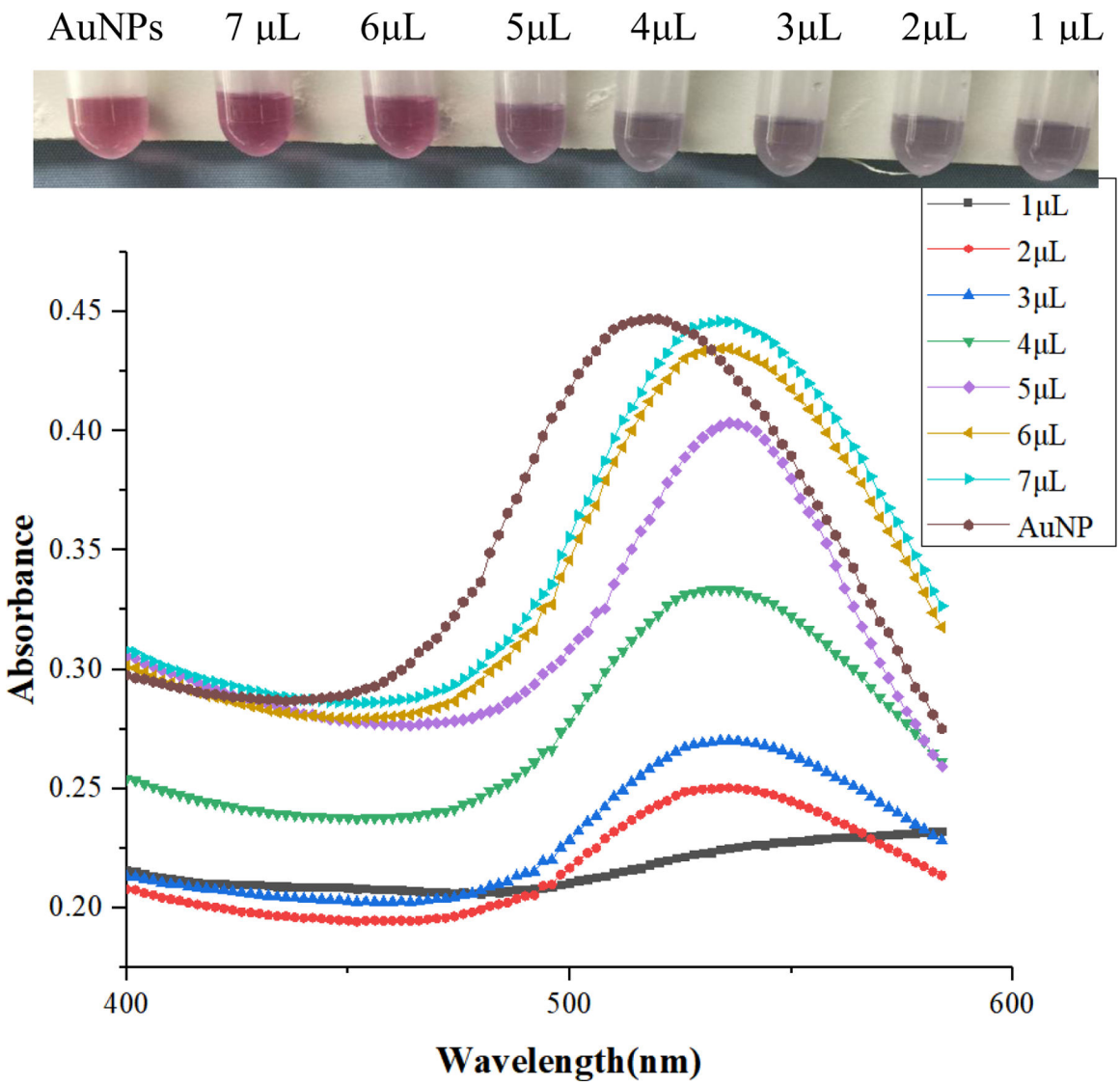

Fig. 3.
Optimization of the concentration of triazophos McAb for AuNPs.

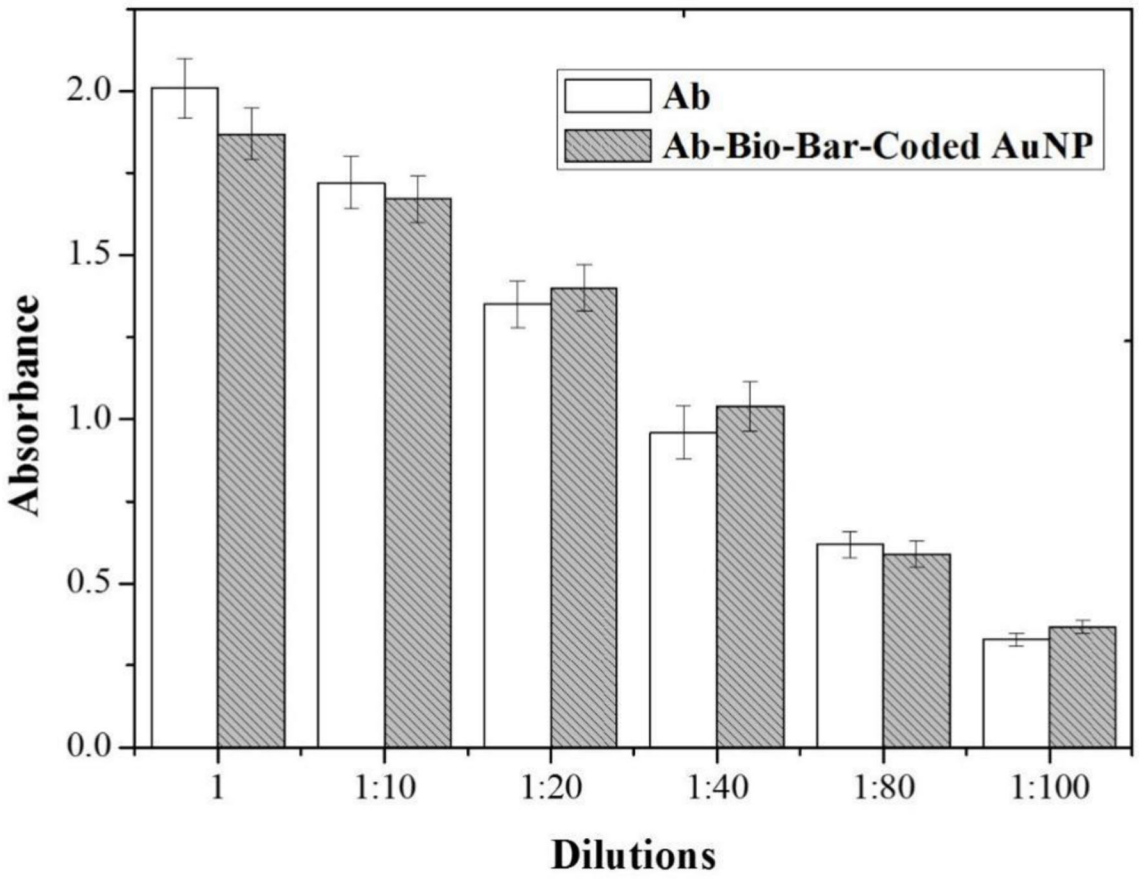

Fig. 4.

The activity of antibody labeled on AuNPs (the initial concentration of antibody was 30.20 μg/mL).

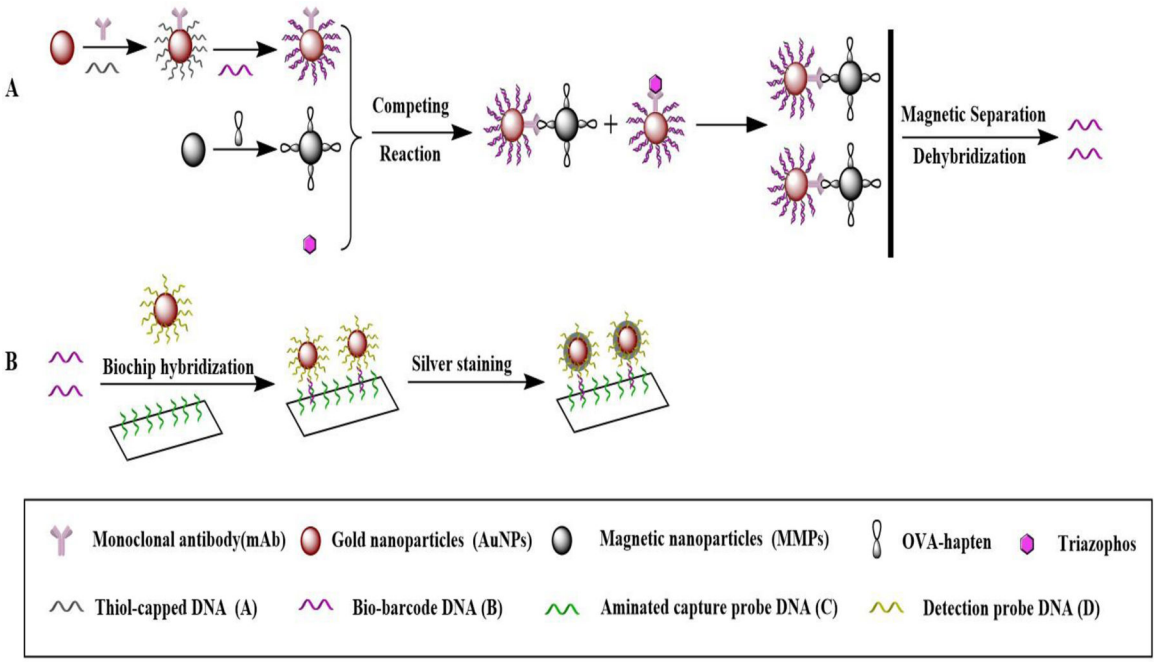

Scheme. 1.

Schematic illustration for detection of triazophos based on biochip and bio-barcode Immunoassay.

Table 1.

Design and synthesis of DNA sequence

Name	DNA Sequence
A	5′-TACGAGTTGAGACCGTTAAGACGAGGCAATCATGCAATCCTG AATGCG-A10-(CH2)6-SH-3′
B	5′-CGCATTCAGGATTGCATGATTGCCTCGTCTTAACGGTCTCAAC TCGTA-3′
C	5′-NH2-(CH2)6-A10-TACGAGTTGAGACCGTTAAGACGA-3′
D	5′-GGCAATCATGCAATCCTGAATGCG-A10-(CH2)6-SH-3′